

## HMFI/SiC – a novel efficient catalyst for green hydrocarbon production *via* bioisobutanol conversion

Alexey G. Dedov,<sup>a,b</sup> Alexander A. Karavaev,<sup>\*a,b</sup> Alexey S. Loktev,<sup>a,b</sup> Petr V. Zemlianski<sup>b</sup>  
Malika N. Vagapova,<sup>a</sup> Konstantin I. Maslakov,<sup>c</sup> Kirill A. Cherednichenko,<sup>b</sup>  
Sergey V. Egazar'yants,<sup>c</sup> Alexey V. Khoroshilov<sup>d</sup> and Pavel I. Ivanov<sup>d</sup>

<sup>a</sup> A. V. Topchiev Institute of Petrochemical Synthesis, Russian Academy of Sciences, 119991 Moscow, Russian Federation. E-mail: aleksankaray@yandex.ru

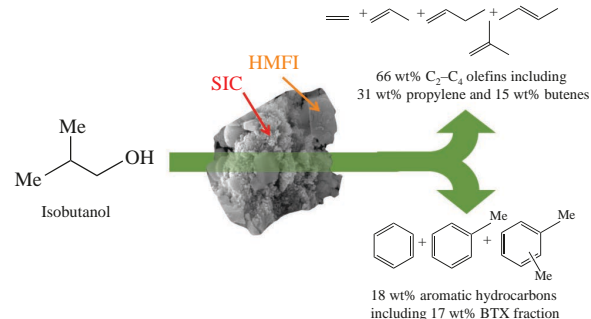
<sup>b</sup> National University of Oil and Gas 'Gubkin University', 119991 Moscow, Russian Federation

<sup>c</sup> Department of Chemistry, M. V. Lomonosov Moscow State University, 119991 Moscow, Russian Federation

<sup>d</sup> D. I. Mendeleev University of Chemical Technology of Russia, 125047 Moscow, Russian Federation

DOI: 10.1016/j.mencom.2023.10.031

Conversion of isobutyl alcohol over the HMFI/SiC composite has been for the first time studied. Isobutanol (bioisobutanol) considered as a promising product of biomass processing was catalytically converted into aromatic hydrocarbons of the benzene–toluene–xylene fraction (BTX) and olefins C<sub>2</sub>–C<sub>4</sub> (mainly propylene and butenes). Compared with the pure zeolite, the incorporation of HMFI into the SiC matrix enhanced the yields of C<sub>2</sub>–C<sub>4</sub> olefins and BTX in the isobutanol conversion due to increased densities of Brønsted and Lewis acid centers.



**Keywords:** isobutanol, HMFI/SiC composite, catalysis, arenes, C<sub>2</sub>–C<sub>4</sub> olefins, propylene, 'green' hydrocarbons.

Olefins C<sub>2</sub>–C<sub>4</sub> and aromatic hydrocarbons, especially the benzene–toluene–xylene fraction (BTX), are basic petrochemicals. They are widely used to produce plastics, synthetic fibers, rubbers, *etc.*<sup>1–3</sup> Oil, natural gas and coal are commonly used raw materials for aromatic hydrocarbons<sup>4</sup> and C<sub>2</sub>–C<sub>4</sub> olefins<sup>1</sup> production. The Paris climate agreement aims at the decarbonization of industry. Twenty countries (including the EU and China) set ambitious goals to achieve carbon neutrality by the middle of the 21<sup>st</sup> century. Therefore, the increased interest has been paid to the development of processes for producing petrochemicals and fuels, including aviation fuel, from renewable ('carbon neutral') raw materials. In addition, the development of efficient catalysts for these processes is very important. Moreover, this approach complies with the principles of green chemistry.

Isobutanol is a promising intermediate product of the processing of plant biomass – a renewable raw material – into petrochemicals.<sup>5–7</sup> Isobutanol production is based on the biotechnological achievements of the team of the Nobel Prize laureate Prof. F. Arnold. They managed to create microorganisms that produce isobutyl alcohol *via* fermentation of carbohydrates with up to 100% efficiency.<sup>8</sup> Gevo<sup>5</sup> and Butamax<sup>6</sup> implemented the production of bioisobutanol. The isobutanol yield of 24 wt% was achieved with a combination of the fermentation and rectification stages.<sup>9</sup>

There is a limited number of publications on the BTX and C<sub>2</sub>–C<sub>4</sub> olefins production by the catalytic conversion of isobutanol. The conversion of isobutyl alcohol over USY, Beta and HMFI zeolites (HMFI – proton form of MFI type zeolite, MFI – structure of modernite form inverted) was studied.<sup>10</sup> A high

total yield of aromatic hydrocarbons of 61.4 wt% was obtained over the HMFI catalyst promoted with 5.1 wt% of Zn. The yield of C<sub>2</sub>–C<sub>4</sub> olefins was 9.3 wt%.

Conversion of isobutanol over unpromoted HMFI zeolite at 550 °C resulted in the predominant production of C<sub>2</sub>–C<sub>4</sub> olefins with a yield of 77.4 wt%.<sup>11</sup> The yield of arenes was 9.5 wt%. The incorporation of 2% of gallium into zeolite increased the yield of aromatic hydrocarbons up to 56.2 wt%.

Transformations of isobutanol over the HMFI, Zn/HMFI, and Ga/HMFI catalysts with the SiO<sub>2</sub>/Al<sub>2</sub>O<sub>3</sub> ratios of 50, 60.1 and 56.3 were also studied.<sup>12</sup> A high yield of aromatic hydrocarbons of 59 wt% was achieved over the Ga/HMFI catalyst at a weight hour space velocity (WHSV) of 1.74 h<sup>–1</sup> at 400 °C. A carbon dioxide flow facilitates achieving a high yield of arenes. Carbon dioxide reacts with hydrogen evolved under dehydrocyclization of the produced butene oligomers.<sup>12</sup> Chemical bonding of released hydrogen shifts the equilibrium toward arene formation.

Recently,<sup>13</sup> we observed the predominant formation of C<sub>2</sub>–C<sub>4</sub> olefins with the yield of 54 wt% in the isobutanol conversion over the nonpromoted HMFI zeolite synthesized by a microwave hydrothermal method.

In this paper, we report for the first time the application of the HMFI/SiC composite as a catalyst of the isobutanol conversion to hydrocarbons. This material was earlier synthesized in the proton form by the microwave hydrothermal method.<sup>14,15</sup> The incorporation of mesoporous chemically inert high thermal conductivity silicon carbide in the composite structure can enhance the heat and mass transfer.

The microwave hydrothermal synthesis of HMFI/SiC in the proton form and its characterization by XRD, SEM, low-

temperature nitrogen physisorption and thermal desorption of ammonia were previously reported.<sup>14,15</sup> The catalytic tests and characterization of the catalyst are described in the Online Supplementary Materials. The synthesis of the composite in the proton form eliminates the long stage of ion exchange during transformation of zeolite into the proton form.

The zeolite content in the composite calculated on the basis of the characteristic bands intensities in its IR spectrum (Figure S1) related to those for pure HMFI zeolite was 77%.

The aluminum and silicon contents in the composite and pure HMFI zeolite synthesized by the same method are compared in Table 1. The  $\text{SiO}_2/\text{Al}_2\text{O}_3$  molar ratio in the zeolite phase of the composite was calculated taking into consideration the presence of silicon in both the zeolite and SiC. It should be noted that the addition of silicon carbide to the synthesis mixture reduced the silica module of the zeolite.

According to the SEM data, the morphologies of the fresh HMFI/SiC catalyst (Figure S2) and spent catalyst regenerated *via* oxidative treatment at 700 °C (Figure 1) are very similar. HMFI zeolite particles of 1–2 microns in size are incorporated into the silicon carbide matrix.

Low-temperature nitrogen physisorption analysis showed that the textural parameters of the spent catalyst after oxidative regeneration are only slightly lower than those of the fresh catalyst (Table S2): both the microporous structure of the HMFI zeolite and the mesopores of the silicon carbide phase were preserved.

The acidic properties of the catalyst measured by  $\text{NH}_3$ -TPD (Table S3) demonstrated that the incorporation of HMFI into SiC increased the content of medium strength acid sites and simultaneously decreased the content of strong acid sites. After the catalytic test and oxidative regeneration, the total amount of acid sites decreased from 202 to 73  $\mu\text{mol g}^{-1}$  and medium strength acid sites predominated in the spent catalyst after regeneration ( $56 \mu\text{mol g}^{-1}$ ).

The results of tests of the HMFI/SiC composite in isobutanol conversion are shown in Figures 2–4 and Table S1. The isobutanol conversion and products yields were calculated using formulas S1–S2. Isobutanol conversion was 100% in all catalytic tests.

At elevated temperatures isobutanol is initially dehydrated over MFI zeolites to form isobutene.<sup>10,11</sup> The resulting isobutene is partially isomerized and the mixture of butenes undergoes oligomerization. Then, the oligomers are either dehydrocyclized to form arenes or cracked to form low-molecular-weight olefins. Cracking products are also capable of oligomerization and further dehydrocyclization.

Figure 2 shows the temperature dependencies of the total yields of  $\text{C}_2$ – $\text{C}_4$  olefins and arenes. The catalyst was tested in both the diluted with nitrogen [Figure 2(a)] and undiluted [Figure 2(b)] isobutanol flows.

In the case of nitrogen-diluted isobutanol [Figure 2(a)], the temperature rise from 400 to 600 °C increased the yield of  $\text{C}_2$ – $\text{C}_4$  olefins from 23 to 66 wt%. The arene yield was 21–23 wt% at 400–500 °C and it decreased to 18 wt% with increasing temperature.

In the tests with undiluted isobutanol the yield of  $\text{C}_2$ – $\text{C}_4$  olefins also increased with temperature [Figure 2(b)], but it was noticeably lower than in the case of nitrogen-diluted isobutanol.

**Table 1** Contents of Al and Si in HMFI zeolite and HMFI/SiC composite.

Sample	Al (wt%)	Si (wt%)	Si/Al molar ratio	$\text{SiO}_2/\text{Al}_2\text{O}_3$ molar ratio in zeolite phase
HMFI	$0.36 \pm 0.04$	$50.9 \pm 0.4$	137	274
HMFI/SiC	$0.58 \pm 0.05$	$47.7 \pm 0.2$	79	122

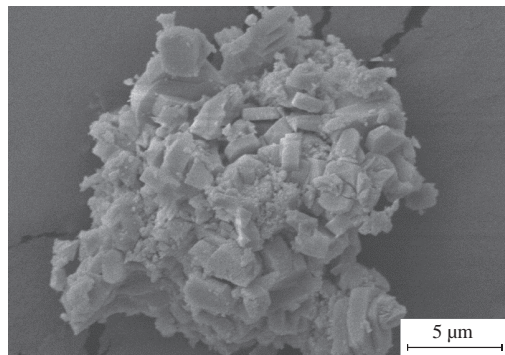


**Figure 1** SEM image of spent HMFI/SiC after regeneration. Magnification 5000 $\times$ .

The maximum arene yield of 30 wt% was observed at 400 °C and it was by 9 wt% higher than that for the test with diluted isobutanol. At 450 °C the yield of arenes decreased to 24 wt% and remained within the range of 21–25 wt% at higher temperatures. An example of the material balance calculation for one of the tests is shown in Table S1.

Dilution of isobutanol with nitrogen may contribute to the displacement of the initially formed  $\text{C}_2$ – $\text{C}_4$  olefins from the reactor, which explains the higher yield of these products compared to undiluted isobutanol. Increasing the temperature accelerates cracking reactions, which also contributes to the increase in the  $\text{C}_2$ – $\text{C}_3$  olefins yield. In the experiments with undiluted isobutanol  $\text{C}_2$ – $\text{C}_4$  olefins are more completely involved in the oligomerization and dehydrocyclization reactions of oligomers. This increases the yield of arenes and decreases the yield of  $\text{C}_2$ – $\text{C}_4$  olefins. The growth of the arene yield by 15 wt% in the *n*-butanol conversion over HMFI when the pressure was increased to 20 bar was reported.<sup>22</sup> In our case, a similar effect may result from the higher partial pressure of isobutanol when it was fed undiluted. The high yield of arenes at a low temperature of 400 °C [Figure 2(b)] is apparently associated with less intensive cracking reactions that lead to the formation of  $\text{C}_2$ – $\text{C}_3$  olefins.

Thus, the supply of nitrogen to the reactor or its absence makes it possible to control the selectivities for the formation and yields of the main isobutanol conversion products. The total yield of the  $\text{C}_2$ – $\text{C}_4$  olefins in the conversion of nitrogen-diluted isobutanol over the HMFI/SiC catalyst reached 66 wt% [Figure 2(a)]. The content of propylene and butenes in the resulting  $\text{C}_2$ – $\text{C}_4$  olefins was high, up to 70 wt% (Table S1). Moreover, the yield of propylene increased with increasing temperature, and with diluting isobutanol with nitrogen, reaching 31 wt%. We managed to achieve a high propylene productivity of 0.846  $\text{g g}_{\text{cat}}^{-1} \text{h}^{-1}$  surpassing the known literature data on the production of propylene *via* isobutanol conversion on zeolites (Figure 3).

When undiluted isobutanol was converted over HMFI/SiC, a higher yield of the BTX fraction was usually achieved. The content of BTX in the produced aromatic hydrocarbons increased

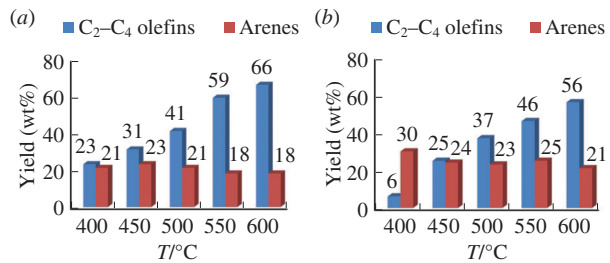


**Figure 2** Temperature dependencies of  $\text{C}_2$ – $\text{C}_4$  olefins and arenes yields in conversion of (a) nitrogen-diluted and (b) nitrogen-undiluted isobutanol flows over HMFI/SiC catalyst. WHSV = 2.2  $\text{h}^{-1}$ ; time-on-stream, 2 h at each temperature.

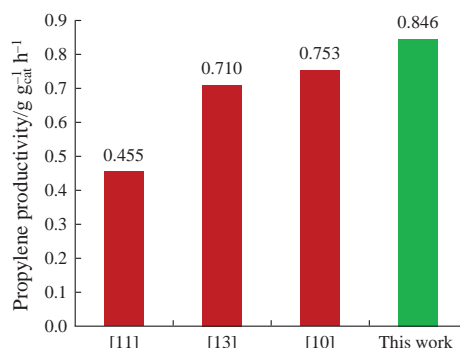


**Figure 3** Propylene productivities in catalytic conversion of isobutanol over catalyst synthesized in this work and reported in literature (refs. 10, 11, 13).

with increasing temperature up to 90–95 wt% both for diluted and undiluted isobutanol conversion.

Our results obviously demonstrate that the incorporation of HMFI zeolite into the SiC matrix enhances the propylene and arenes productivities in the isobutanol conversion (Figure 4). However, the isobutanol conversion over pure SiC shows only partial dehydration and isomerization reactions and probably proceeds *via* non-catalytic thermal processes (Table S4).

The HMFI/SiC composite demonstrated the stability of phase composition, textural properties and morphology. Its higher efficiency in the isobutanol conversion in comparison with pure HMFI zeolite synthesized by the same method probably occurred due to their different acidic properties.

According to the data of the Fourier transform infrared spectroscopy (FTIR) of adsorbed pyridine (Table 2), the contents of Brønsted acid centers ( $82 \mu\text{mol g}^{-1}$ ) and Lewis acid centers ( $22 \mu\text{mol g}^{-1}$ ) in HMFI/SiC were higher than those in the pure HMFI zeolite. Taking into account the zeolite content in the composite estimated from the IR spectra, the numbers of Brønsted and Lewis acid centers were recalculated relative to the mass of zeolite in the composite. The recalculated values are  $106 \mu\text{mol g}^{-1}$  for Brønsted acid centers and  $29 \mu\text{mol g}^{-1}$  for Lewis acid centers.

Thus, the introduction of silicon carbide at the stage of zeolite synthesis made it possible to produce a composite containing zeolite with the increased total content of acid centers provided by higher numbers of both Brønsted and Lewis acid centers. The increase in the content of Brønsted acid centers could result from the increased amount of lattice aluminum in the zeolite framework (see Table 1), while the elevated concentration of Lewis acid centers can be associated with the increase in defectiveness of the zeolite structure and its decrease in the silica module. Thus, the higher arene and olefin yields over the composite, in our view, may be related to the higher contents of

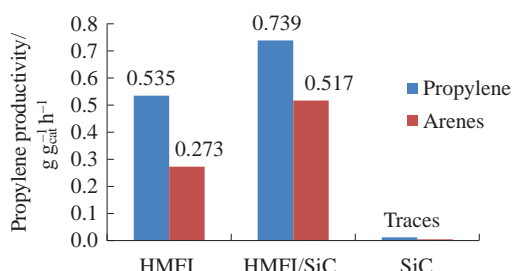


**Figure 4** Propylene and arene productivities in catalytic conversion of isobutanol over SiC, HMFI zeolite and HMFI/SiC at  $550^\circ\text{C}$ , WHSV =  $2.2 \text{ h}^{-1}$ . The productivities over HMFI zeolite and HMFI/SiC composite were calculated based on the mass of zeolite phase, while the same data for SiC were calculated based on the SiC mass.

**Table 2** Brønsted and Lewis acidity of HMFI zeolite and HMFI/SiC composite.

Sample	Brønsted acidity/ $\mu\text{mol g}^{-1}$	Lewis acidity/ $\mu\text{mol g}^{-1}$
HMFI	74	13
HMFI/SiC	82	22
HMFI/SiC (recalculated to HMFI mass in composite)	106	29

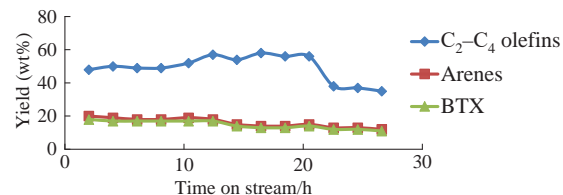


**Figure 5**  $\text{C}_2\text{--}\text{C}_4$  olefins, arenes and BTX yields vs. time-on-stream in undiluted isobutanol conversion over HMFI/SiC composite at  $600^\circ\text{C}$ . WHSV =  $2.2 \text{ h}^{-1}$ .

Brønsted and Lewis acid centers in the composite compared to those in the pure HMFI zeolite.

Figure 5 shows the changes in the yields of  $\text{C}_2\text{--}\text{C}_4$  olefins, arenes and BTX vs. time-on-stream in the isobutanol conversion over the HMFI/SiC catalyst. HMFI/SiC demonstrated a stable yield of  $\text{C}_2\text{--}\text{C}_4$  olefins during 20 h. The yields of arenes and BTX did not change significantly up to 12 h and then slightly decreased.

Summarizing, we have revealed high efficiency of the HMFI/SiC composite catalyst in the conversion of isobutanol into aromatic hydrocarbons and  $\text{C}_2\text{--}\text{C}_4$  olefins. This composite was directly synthesized in the proton form by the microwave hydrothermal method. The HMFI/SiC catalyst demonstrated a high propylene yield (31 wt%) in the isobutanol conversion and the highest propylene productivity of  $0.846 \text{ g}_{\text{cat}} \text{ h}^{-1}$  among all known catalysts of isobutanol conversion.<sup>23</sup> Additionally, the synthesized material allows producing aromatic hydrocarbons with the yield of up to 21–30%. The content of the BTX fraction in aromatic hydrocarbons reaches 90–95%. The catalyst also showed relatively high stability in the tests. The results thus demonstrate the promising properties of the HMFI/SiC composite in the catalytic conversion of isobutanol, including the conversion of biogenic isobutanol into green petrochemicals and fuel components.

This research was carried out within the state funding of TIPS RAS. The authors thank RFBR (project no. 20-03-00492) for financial support. The authors express their gratitude to SICAT for the silicon carbide samples provided. The analytical studies of catalysts by ICP-OES method were carried out at the D. I. Mendeleev Center for Collective Use of Scientific Equipment.

#### Online Supplementary Materials

Supplementary data associated with this article can be found in the online version at doi: 10.1016/j.mencom.2023.10.031.

#### References

- 1 V. Zacharopoulou and A. A. Lemonidou, *Catalysts*, 2018, **8**, 2.
- 2 R. Geyer, J. R. Jambeck and K. L. Law, *Sci. Adv.*, 2017, **3**, e1700782.
- 3 C. M. Lok, J. Van Doorn and G. A. Almansa, *Renewable Sustainable Energy Rev.*, 2019, **113**, 109248.
- 4 G. Busca, *Energies*, 2021, **14**, 4061.
- 5 Decarbonized Fuels and Chemicals, <https://gevo.com/>.
- 6 bp America, Press Releases and Public Statements, 2017, [https://www.bp.com/en\\_us/united-states/home/news/press-releases/bp-and-dupont-joint-venture-butamax-acquisition-of-ethanol-facility-in-kansas.html?ysclid=la9j8d2eta991679985](https://www.bp.com/en_us/united-states/home/news/press-releases/bp-and-dupont-joint-venture-butamax-acquisition-of-ethanol-facility-in-kansas.html?ysclid=la9j8d2eta991679985).

7 A. G. Dedov, A. A. Karavaev, A. S. Loktev and A. K. Osipov, *Pet. Chem.*, 2021, **61**, 1139 (*Neftekhimiya*, 2021, **61**, 716).

8 S. Bastian, X. Liu, J. T. Meyerowitz, C. D. Snow, M. M. Y. Chen and F. H. Arnold, *Metab. Eng.*, 2011, **13**, 345.

9 C. Ryan, *Gevo Overview. Large Scale Drop-Ins from Renewable Olefins. World Congress on Industrial Biotechnology*, Montreal, Canada, 2017, Presentation.

10 L. Yu, S. Huang, S. Zhang, Z. Liu, W. Xin, S. Xie and L. Xu, *ACS Catal.*, 2012, **2**, 1203.

11 Z.-Y. Du, B.-B. Zhang, T.-S. Chen, Y. Betancur and W.-Y. Li, *Energy Fuels*, 2019, **33**, 10176.

12 Y.-H. Mo, Y.-Ju Choi, H. Choi and S.-E. Park, *Res. Chem. Intermed.*, 2017, **43**, 7223.

13 A. G. Dedov, A. A. Karavaev, A. S. Loktev, A. S. Mitinenko and I. I. Moiseev, *Catal. Today*, 2021, **367**, 199.

14 I. I. Moiseev, A. S. Loktev, E. A. Isaeva, A. S. Mitinenko, A. A. Karavaev and A. G. Dedov, *Patent RU 2725586*, 2020.

15 A. G. Dedov, A. A. Karavaev, A. S. Loktev, A. S. Mitinenko, K. A. Cherednichenko and I. I. Moiseev, *Mater. Lett.*, 2021, **290**, 129497.

16 Y. Liu, S. Podila, D. L. Nguen, D. Edouard, P. Nguen, C. Pham, M. J. Ledoux and C. Pham-Huu, *Appl. Catal., A*, 2011, **409–410**, 113.

17 X. Ou, C. Wu, K. Shi, C. Hardacre, J. Zhang, Y. Jiao and X. Fan, *Appl. Catal., A*, 2020, **599**, 117626.

18 Z. Liu, C. Shi, D. Wu, S. He and B. Ren, *J. Nanotechnol.*, 2016, 1486107.

19 Y. C. Kim, J. Y. Jeong, J. Y. Hwang, S. D. Kim and W. J. Ki, *J. Porous Mater.*, 2009, **16**, 299.

20 J. Pérez-Ramírez, D. Verboekend, A. Bonilla and S. Abelló, *Adv. Funct. Mater.*, 2009, **19**, 3972.

21 K. R. Ramasamy and Y. Wang, *J. Energy Chem.*, 2013, **22**, 65.

22 V. C. S. Palla, D. Shee and S. K. Maity, *ACS Sustainable Chem. Eng.*, 2020, **8**, 15230.

23 A. A. Karavaev, A. G. Dedov, A. S. Loktev and P. V. Zemlyanskii, *Patent RU 2768153*, 2022.

Received: 13th June 2023; Com. 23/7190